J. Fluid Mech. (1982), *vol.* 117, *pp.* 27–43
Printed in Great Britain

Magnetic levitation of liquid metals

By A. J. MESTEL

Department of Applied Mathematics and Theoretical Physics,
Silver Street, Cambridge

(Received 12 February 1981 and in revised form 10 December 1981)

The process of levitation melting of metals is examined analytically and numerically for the case of axisymmetric toroidal high-frequency currents. The governing equations for the mean-velocity field and associated free-surface shape are derived under the assumption of low magnetic Reynolds number and the neglect of thermal effects. The form of the solution for high Reynolds number is discussed in general, and particularized to the case of high surface tension, in which limit a perturbation analysis about a spherical shape is presented. Finite-difference techniques are used to solve the Navier–Stokes equations in the sphere, and the surface perturbation is calculated. The asymptotic behaviour of the potential vorticity is illustrated by the numerical experiments.

0. Introduction

When a conductor is placed in an alternating, non-uniform magnetic field $\mathscr{R}(\mathbf{B}e^{i\Omega t})$, where $\mathscr{R}$ denotes the real part, eddy currents $\mathscr{R}(\mathbf{j}e^{i\Omega t})$ are induced in it. The associated Lorentz force density will in general have both a steady component and one fluctuating with frequency 2Ω. If the field is sufficiently strong with respect to gravity levitation may occur, and a time-averaged equilibrium will be reached when the region V occupied by the conductor is such that

$$\int_V (\tfrac{1}{2}\mathscr{R}(\mathbf{j}\wedge\mathbf{B}^*)+\rho\mathbf{g})\,dV = 0, \tag{0.1}$$

where ρ is the density of the conductor, $\mathbf{g}$ is the gravitational acceleration and * denotes the complex conjugate. For a solid conductor, henceforth assumed to be a metal, $\mathbf{B}$ obeys a diffusion equation

$$i\Omega\mathbf{B} = \lambda\nabla^2\mathbf{B}, \tag{0.2}$$

where λ is the magnetic diffusivity, and thus

$$\mathbf{j} = \frac{1}{\mu}\nabla\wedge\mathbf{B} \sim \frac{\Omega B_0}{\mu\lambda}L, \tag{0.3}$$

where μ is the magnetic permeability, B_0 is a typical value of $\mathbf{B}$, and L its length scale of variation inside V. Equation (0.1) therefore implies

$$\frac{B_0^2}{\mu}\frac{L^2\Omega}{\lambda} \sim \rho g a, \tag{0.4}$$

where a is a length scale of V. The field strength required can thus be reduced by increasing Ω. Eventually, as is well known, an asymptotic state is reached in which $L^2 \sim \lambda/\Omega$, and the field is confined to a skin layer near the surface.

Inevitably associated with the Lorentz force is an Ohmic heating rate

$$E = \int_V \mathbf{j}^2 \mu\lambda \, dV \sim \frac{B_0^2}{\mu} a^2 \lambda^{\frac{1}{2}} \Omega^{\frac{1}{2}} \tag{0.5}$$

(in the asymptotic state). If Ω is sufficiently large, therefore, the levitated metal will begin to melt. This process is known as 'levitation melting', or 'the electromagnetic crucible'.

Levitation melting of metals was first suggested by Muck (1923) in a German patent, but it was some years later that the first experimental work was published by Okress *et al.* (1952). Since then, many suitable levitation coils have been found by Polonis (Polonis & Parr 1954) and others, extensive references to which are given by Peifer (1965). The greatest interest in levitation techniques has been shown by metallurgists, for whom the advantages of non-contamination from the crucible, efficient stirring and rapidity of melting make them superior to more-conventional crucible melting, when a pure homogeneous melt is required.

Once the metal has melted a number of changes occur. Firstly, the fluid surface is free to adjust according to the stresses upon it, and the suspended blob of fluid will adopt a shape which is unknown *a priori*. Secondly, we observe that the Lorentz force is in general rotational and so necessarily drives rotational fluid motions, the Reynolds number for which is large ($\sim 10^4$ for a free-fall velocity, $a = 0{\cdot}01$ m and a kinematic viscosity $\sim 10^6$ m^2/s). Finally there is the possibility of magnetic induction bending the field lines in V.

The greatest difficulty facing levitation melting is the maintenance of stability of the suspended blob. The possible instabilities are essentially either global, or local to the surface. The global instabilities, which cause the metal to move as a whole, must be prevented by carefully choosing the external current distribution that generates the supporting field so that the blob is close to a local field minimum. The simplest method of ensuring this, used in all of the coil designs cited above, is to arrange a basket of axisymmetric coils wound in the same sense with one or two counter-windings at the top to provide a 'crucible lid'. The disadvantage of an axisymmetric design is that along the axis of symmetry the Lorentz force is zero, and hence we must rely on surface tension to provide the necessary support against hydrostatic pressure there. As a result, the blob tends in practice to adopt a conical shape with its apex pointing downwards. Not more than about 50 g of liquid has been levitated in this manner, greater masses tending to drip down the central axis. This dripping tendency is an example of a surface instability. Harris & Stephan (1975) have examined other surface distortions, using sodium in an oil of slightly lower density, but it is not clear that the oil motions are negligible, and thus direct comparison is difficult. Sagardia (1977) has levitated 1 kg of aluminium by means of multifrequency non-axisymmetric coils. There being no time-averaged interaction between different frequencies, it is possible to add the magnetic pressures due to each frequency. Thus along the axis of one set of coils, others may be called upon to give support.

In this paper we attempt an analytical and numerical study of the levitation

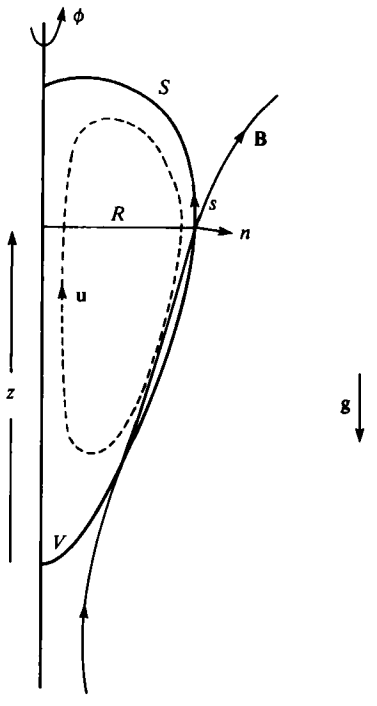

FIGURE 1. General co-ordinate system.

phenomenon with the aim of understanding the relation between the external coil arrangement, the adopted surface shape and the internal fluid flow. We confine ourselves to the axisymmetric, single-frequency case, which is more amenable to analysis. We ignore all thermal effects, assuming an equilibrium temperature has been reached, or that variations with temperature (of viscosity, say) are slow. Buoyancy forces are proportional to density differences and are therefore negligible compared with the Lorentz force, which, by (0.1), is proportional to the total density. We are also going to assume that the flow is essentially laminar, by which we mean that turbulent effects (if any) can be represented by an effective 'eddy viscosity' to replace the molecular viscosity. This is our most severe assumption, as laboratory liquid-metal flows are usually turbulent, and this can only be partially modelled by an eddy viscosity. Nevertheless, for analytical progress, some such assumption must be made.

In §1 we derive the magnetic field inside the metal. In §§2 and 3 we discuss the flow for a general surface, and particularize in §4 to the limit of high surface tension. In §5 we describe the numerical experiments performed in this limit.

1. The magnetic field

We assume a given axisymmetric toroidal current distribution $\mathscr{R}(\mathbf{j}_0 e^{i\Omega t})$ surrounding a volume V of liquid metal bounded by a surface S, whose shape is known. We define locally to the surface an orthogonal co-ordinate system (n, s, ϕ) as in figure 1, where ϕ is the azimuthal angle and n, s are the normal and tangential co-ordinates on S.

The poloidal magnetic field in V, $\mathscr{R}(\mathbf{B}e^{i\Omega t})$, obeys the induction equation

$$i\Omega\mathbf{B} = \nabla\wedge(\mathbf{u}\wedge\mathbf{B}) + \lambda\nabla^2\mathbf{B}, \tag{1.1}$$

where $\mathbf{u}$ is the fluid velocity and λ the magnetic diffusivity. The magnetic Reynolds number $R_m = U_0 L/\lambda$, where U_0 and L are scales of velocity and field variation, we take to be small. This assumption is certainly valid for high-enough frequency, since not only does $L\to 0$ as $\Omega^{-\frac{1}{2}}$, but also, as we shall see, $U_0\to 0$ as $\Omega^{-\frac{1}{2}}$. The range of consistency of this approximation will be checked later. It results in the neglect of the fluidity of the metal, and we are left with the standard problem of field penetration into a solid conductor. If we write $\mathbf{B} = \nabla\wedge(0,0,A)$ (1.1) becomes

$$\frac{i\Omega}{\lambda}A = \left(\nabla^2 - \frac{1}{R^2}\right)A. \tag{1.2}$$

As $\Omega\to\infty$ we obtain the asymptotic solution by taking $\partial/\partial n \gg \partial/\partial s$

$$A = 2\delta B_s(s)\exp\left[(1+i)\frac{n}{2\delta}\right] + O(\delta^2), \tag{1.3}$$

where $\delta = (\lambda/2\Omega)^{\frac{1}{2}}$ is the skin depth. $B_s(s)$ is obtained by matching with the external problem

$$\nabla\wedge\mathbf{B} = \mu_0\mathbf{j}_0, \quad \nabla.\mathbf{B} = 0, \quad \mathbf{B}\to 0 \quad \text{as} \quad |\mathbf{x}|\to\infty. \tag{1.4}$$

Equation (1.4), together with the boundary condition $B_n = O(\delta)$ on S, can be solved for B_s by means of an integral equation over S involving a Greens function.

Then inside V, to lowest order in δ, we have

$$\mathbf{B} = \left(\frac{2\delta}{R}\frac{\partial}{\partial s}(RB_s), -(1+i)B_s, 0\right)\exp\left[(1+i)\frac{n}{2\delta}\right], \tag{1.5}$$

the current

$$\mathbf{j} = \left(0, 0, -\frac{iB_s}{\delta\mu}\right)\exp\left[(1+i)\frac{n}{2\delta}\right], \tag{1.6}$$

and the time-averaged Lorentz force per unit mass

$$\mathbf{F} = \tfrac{1}{2}\mathscr{R}(j\wedge B^*) = \left(-\tfrac{1}{2}|B_s|^2, \delta\mathscr{I}\left\{B_s\frac{\partial B_s^*}{\partial s}\right\}, 0\right)\frac{e^{n/\delta}}{\delta\mu\rho}, \tag{1.7}$$

where ρ is the (constant) fluid density and $\mathscr{I}$ denotes the imaginary part. Now if the applied currents are single-phased (i.e. if $\mathbf{j}_0 = \mathbf{j}_{0r}e^{i\alpha}$, $\mathbf{j}_{0r}$ real, α real and constant) then by a suitable choice of time origin we may take B_s to be real, and thus $\mathscr{I}\{B_s\partial B_s^*/\partial s\} = O(\delta)$. If we assume this to be the case (as such currents are invariably used in practice) we can express $\mathbf{F}$ and $\mathbf{G} = \nabla\wedge\mathbf{F}$ to leading order as

$$\mathbf{F} = -\frac{B_s^2}{2\mu\rho}\frac{1}{\delta}e^{n/\delta}(1,0,0), \tag{1.8}$$

$$\mathbf{G} = \frac{B_s}{\mu\rho\delta}\frac{\partial B_s}{\partial s}e^{n/\delta}(0,0,1), \tag{1.9}$$

as given by Sneyd (1979). Should the currents be multiphased, however, then if we write $B_s = B_{sr} + iB_{si}$ with B_{sr}, B_{si} real there exists an additional tangential force

$$\mathbf{F}_{\text{mult}} = \frac{1}{\mu\rho}\left(B_{si}\frac{\partial B_{sr}}{\partial s} - B_{sr}\frac{\partial B_{si}}{\partial s}\right)e^{n/\delta}\,(0,1,0). \tag{1.10}$$

We shall return to this point later, but for the moment confine ourselves to considering the fluid motions driven by $\mathbf{F}$ inside V, still regarding the surface S as fixed.

2. The velocity field

We are going to seek a steady laminar axisymmetric poloidal velocity field. Sneyd (1979) has shown that only for infinite cylinders is the rotational part of the Lorentz force, and hence the velocity field, truly steady. We must therefore show the time-dependent part of the velocity to be negligible.

The inviscid vorticity equation for $\boldsymbol{\omega} = \nabla \wedge \mathbf{u}$ is

$$\frac{\partial \boldsymbol{\omega}}{\partial t} = \nabla \wedge (\mathbf{u} \wedge \boldsymbol{\omega}) + \mathbf{G} + \mathbf{G}', \tag{2.1}$$

where $\mathbf{G}'$ is the contribution from the fluctuating Lorentz force and is of the same order as $\mathbf{G}$. We define a suitable large scale time-average $\overline{\ }$ and write $\boldsymbol{\omega}(\mathbf{x}, t) = \overline{\boldsymbol{\omega}}(\mathbf{x}) + \boldsymbol{\omega}'$, where $\overline{\boldsymbol{\omega}}' = 0$.

Now the assumption of low magnetic Reynolds number is equivalent to stating $\partial/\partial t \gg \mathbf{u}.\nabla$. The fluctuating part of (2.1) then reduces to

$$\frac{\partial \boldsymbol{\omega}'}{\partial t} = \mathbf{G}' + O(R_{\text{m}}), \tag{2.2}$$

or $\boldsymbol{\omega}' \sim \mathbf{G}/\Omega$. The steady part of (2.1) is

$$\nabla \wedge (\overline{\mathbf{u}} \wedge \overline{\boldsymbol{\omega}}) + \nabla \wedge (\overline{\mathbf{u}' \wedge \boldsymbol{\omega}'}) + \mathbf{G} = 0. \tag{2.3}$$

Now
$$\frac{|\nabla \wedge (\overline{\mathbf{u}' \wedge \boldsymbol{\omega}'})|}{|G|} \sim \frac{\omega'^2}{G} \sim \frac{G}{\Omega^2}. \tag{2.4}$$

We therefore see the effects of fluctuation are negligible provided $G/\Omega^2 \ll 1$, or from (1.9) and (0.1), $g/\Omega^2 \ll \delta$. This is equivalent to saying that the free-fall distance over one period must be considerably smaller than the scale of field variation. For Ω as low as 100 Hz. $g/\delta\Omega^2 \sim 0{\cdot}05$ for $\lambda = 0{\cdot}1$ m^2/s, $g = 10$ m/s^2. The addition of small viscosity, though important to the flow as a whole, does not affect the above analysis. It is thus correct to suppose the laminar velocity field to be steady, as suggested by Moffatt (1965).

The velocity $\mathbf{u}(\mathbf{x})$ and pressure $p(\mathbf{x})$ thus obey the steady, incompressible Navier–Stokes equations in V

$$\mathbf{u}.\nabla\mathbf{u} = -\nabla(p/\rho + gz) + \mathbf{F} + \nu\nabla^2\mathbf{u}, \tag{2.5}$$

$$\nabla.\mathbf{u} = 0, \tag{2.6}$$

where ν is the kinematic viscosity and z a vertical co-ordinate. The associated vorticity equation is

$$\nabla \wedge (\mathbf{u} \wedge \boldsymbol{\omega}) + \mathbf{G} + \nu\nabla^2\boldsymbol{\omega} = 0. \tag{2.7}$$

The boundary conditions on the stationary free surface S are

$$u_i n_i = 0, \quad s_i e_{ij} n_j = 0, \quad p = \gamma K, \qquad (2.8), (2.9), (2.10)$$

where

$$e_{ij} = \frac{1}{2}\left\{\frac{\partial u_i}{\partial x_j} + \frac{\partial u_j}{\partial x_i}\right\}$$

is the rate-of-strain tensor, n_i, s_i the unit normal and tangent vectors, γ the surface tension, and K the curvature of the surface, most easily defined as $\partial n_i/\partial x_i$.

For this high-Reynolds-number flow we have neglected the normal viscous stress in (2.10) in favour of the pressure. Some discussion, however, is required as to the applicability of the tangential stress-free condition (2.9) to liquid metals. Some metals, notably mercury and aluminium are invariably found in air with a solid oxide coating or 'skin'. There is thus some justification for using here instead a no-slip condition as used by Moffatt (1977) and Sneyd (1979). However, these works are mainly directed towards the problem of electromagnetic stirring of a cylindrical column of cooling metal, in which the melt is deliberately allowed to solidify on the outside. In our case the stronger fields required by the levitation constraint (0.1) would cause larger viscous stresses on a solid surface, which are likely to break up any such skin. Indeed, Okress *et al.* (1952) record seeing islands of film floating on levitated aluminium. If the levitation occurs in an inert atmosphere the problem does not arise.

If we write $\mathbf{u} = (u_n, u_s, 0)$, $\boldsymbol{\omega} = (0, 0, \omega)$ then (2.8) and (2.9) can be rewritten

$$u_n = 0, \quad \omega = 2cu_s, \qquad (2.11)$$

where c is the one-dimensional curvature of the surface intersected with an axial plane, related to K by the formula

$$K = c + \frac{1}{R}\left(1 + \left(\frac{dR}{dz}\right)^2\Big|_S\right)^{-\frac{1}{2}}, \qquad (2.12)$$

where R is the distance from the axis of symmetry.

We intend to eliminate p from the problem by dealing with the vorticity equation. We therefore re-express (2.10) as follows. Integrating (2.5) along a surface streamline we obtain, using (2.8) and (2.10)

$$\frac{\gamma K}{\rho} + gz + \tfrac{1}{2}u_s^2 - \nu\int_0^s \frac{1}{R}\frac{\partial}{\partial n}(R\omega)\Big|_{n=0} ds = \frac{\gamma K_0}{\rho}, \qquad (2.13)$$

where K_0 is the curvature at the bottom ($s = 0$). It should be noted with reference to (1.10) that were the external currents *double*-phased there would exist another term in (2.13) of the same order as the gravitational one, which could be important in determining the surface shape.

The importance of surface tension can be seen by evaluating (2.13) at the top of the blob. If we ignore the viscous term we obtain, as given by Polonis (1954)

$$\frac{\gamma}{\rho}(K_0 - K_t) = gh, \qquad (2.14)$$

where K_t is the curvature at the top, and h the total height. This limits the total amount of metal levitatable by an axisymmetric device of the type we are considering, as the thinning required for high curvature at the bottom will probably render the

system prone to surface tension instabilities, or alternatively increase the required height of the levitation apparatus to an inconvenient level.

For a given surface S, (2.5), (2.6) with (2.11) are sufficient to determine $\mathbf{u}$ throughout V. Equation (2.13) is an additional constraint that the surface must satisfy for equilibrium.

3. Scaling

Let us formally define

$$a = \left(\frac{3v}{4\pi}\right)^{\frac{1}{3}} \tag{3.1}$$

where v is the volume of V. We expect three distinct regions of the flow: a core region of length scale a, free from rotational forces; a magnetic skin layer of thickness $a\delta_{\mathrm{m}}$, in which the Lorentz force acts, and thirdly, a weak viscous boundary layer of thickness $a\delta_{\mathrm{v}}$, where we have written

$$Re = U_0 a/\nu, \quad \delta_{\mathrm{v}} = Re^{-\frac{1}{2}}, \quad \delta_{\mathrm{m}} = \delta/a. \tag{3.2}$$

Re is of course the Reynolds number for the core flow.

The viscous boundary layer at a free surface plays a minor role. Across it there is an $O(1)$ change in ω and e_{ij}, but the velocity is approximately constant. As a result, there is negligible energy dissipation in this layer.

Across the magnetic layer there is a jump in stress known as the magnetic pressure. If $\delta_{\mathrm{m}} \gg \delta_{\mathrm{v}}$ then this indeed provides a jump in the fluid pressure. If $\delta_{\mathrm{m}} \ll \delta_{\mathrm{v}}$ then it is the viscous stress that jumps and there is a low-Reynolds-number region of thickness $a\delta_{\mathrm{m}}$ within the viscous layer. This must be taken into account when scaling the normal derivative in the surface viscous term in (2.13).

We represent the levitation constraint (0.1) by

$$\alpha = \frac{B_0^2}{2\mu\rho g a}, \tag{3.3}$$

where α is an $O(1)$ constant dependent only on the geometry of the set-up. We define a Weber number as a measure of surface tension

$$W = \frac{\gamma}{\rho g a^2}. \tag{3.4}$$

The rate of energy dissipation can be obtained from (2.5)

$$\int_V \mathbf{u}.\mathbf{F}\, dV = 2\nu \int_V e_{ij} e_{ij}\, dV. \tag{3.5}$$

Now since $\mathbf{F}$ has only a normal component and in the magnetic layer $u_n \sim U_0 \delta_{\mathrm{m}}$, this suggests the scaling

$$U_0 \sim \frac{B_0^2}{2\mu\rho}\frac{\delta}{\nu}. \tag{3.6}$$

This estimate for the velocity magnitude has also been obtained by Sneyd & Moffatt (1982) by means of a streamline integral. It should be noted, however, that this estimate may be too large as the integral on the left-hand side of (3.5) could be

small. Equation (3.6) is stating that the viscous and magnetic forces are of the same magnitude *locally*, whereas (3.5) requires only an *average* equality.

If we non-dimensionalize $\mathbf{u}$, $\mathbf{B}$, $\mathbf{x}$, with respect to U_0, B_0 and a respectively, then from (2.7) we obtain

$$Re\,\nabla\wedge(\mathbf{u}\wedge\boldsymbol{\omega})+\frac{1}{\delta_m}\mathbf{G}+\nabla^2\boldsymbol{\omega}=0. \tag{3.7}$$

Equation (2.13) becomes in non-dimensional form

$$W(K-K_0)+z+\tfrac{1}{2}\alpha\,Re\,\delta_m u_s^2-\frac{\alpha\delta_m}{\min(\delta_m,\delta_v)}\int_0^s\left.\frac{\partial\omega}{\partial y}\right|_{y=0}ds=0, \tag{3.8}$$

where $y=\min(\delta_m,\delta_v)n$ is an $O(1)$ co-ordinate on the surface (inside *both* boundary layers). Equation (2.6) and (2.11) remain unchanged.

In (3.8), if $\delta_m\gg\delta_v$, the integral term is smaller by a factor of δ_v than the u^2 term. If $\delta_m\ll\delta_v$, the integral term in $O(1)$ and in fact becomes the magnetic pressure $\frac{1}{2}\alpha B_s^2$. Thus in either of these limits, to leading order it would be correct to write

$$W(K-K_0)+z+\tfrac{1}{2}\alpha\,Re\,\delta_m u_s^2+\tfrac{1}{2}\alpha B_s^2=O(\delta_m,\delta_v), \tag{3.9}$$

which is a simple physical balance of pressure forces. Equation (3.9) can be shown to be uniformly valid over variations in the ratio of the boundary layer thicknesses, provided the velocity u_s is measured *outside* both layers. Equation (3.8) does not involve any boundary-layer approximations, and may be of more use in numerical work.

We have thus formulated the problem in terms of three dimensionless parameters: Re, δ_m and W. These parameters, repeated here,

$$W=\frac{\gamma}{\rho g a^2},\quad \delta_m=\left(\frac{\lambda}{2\Omega a^2}\right)^{\frac{1}{2}},\quad Re=\frac{\alpha g a^2}{\nu^2}\left(\frac{\lambda}{2\Omega}\right)^{\frac{1}{2}}, \tag{3.10}$$

may in principle be varied independently, by suitable variation of Ω, and two fluid properties, say ρ and ν. Of course not all points in parameter space will be physically accessible, and we now estimate these parameters for a realistic case.

Order-of-magnitude values of the relevant physical constants for liquid metals are

$$\gamma=1\ \mathrm{N/m},\quad \lambda=0{\cdot}1\ \mathrm{m^2/s},\quad \rho=10^4\ \mathrm{kg/m^3}, \tag{3.11}$$

and thus if we take $\Omega=10^6$ Hz, $a=0{\cdot}01$ m and use a *molecular* viscosity $\nu=10^{-6}\,\mathrm{m^2/s}$, the parameters become

$$W=0{\cdot}1,\quad \delta_m=0{\cdot}02,\quad Re=2\times10^5\alpha. \tag{3.12}$$

Now for self-consistency of the scaling we cannot have one term in (3.8) outbalancing all the others. We require therefore

$$Re\,\delta_m\lesssim\max(1,W). \tag{3.13}$$

This constraint on the validity of our scaling is satisfied in either of the limits of high frequency ($\delta_m\to0$) and of high surface tension ($W\to\infty$), but not in the limit of high Reynolds number ($Re\to\infty$). In either of the two former limits the surface shape may be determined independently of the fluid velocity, which greatly simplifies the problem. Now (3.13) is clearly not satisfied by the parameters in (3.12). It becomes so,

however, not only if we consider smaller blobs of fluid or much higher frequencies, but also if we replace the molecular viscosity by a larger turbulent 'eddy viscosity' as may be applicable in certain flow regimes.

We are now in a position to examine more carefully the assumption in §1 of low magnetic Reynolds number. In (1.1)

$$\frac{|\nabla\wedge(\mathbf{u}\wedge\mathbf{B})|}{|\lambda\nabla^2 B|}\sim\frac{\delta_{\mathrm{m}}U_0B_0/\delta}{\lambda B_0/\delta^2}\sim\alpha\frac{ga^3}{\nu\lambda}\delta_{\mathrm{m}}^3, \tag{3.14}$$

and thus with the values of (3.11) the effective magnetic Reynolds number, $R_{\mathrm{m\,eff}}=10^{-3}\alpha$. This is an order of δ_{m} smaller than R_{m} as defined previously since $\mathbf{u}$ and $\mathbf{B}$ are almost parallel in the region where $\mathbf{B}\neq 0$. We thus see that even in the unfavourable parameter range the assumption $R_{\mathrm{m\,eff}}\ll 1$ is eminently reasonable.

We conclude this section with some general remarks about the form of the velocity field, assuming (3.13) to hold, i.e. that the viscous forces are locally of the same magnitude as the Lorentz forces in the magnetic boundary layer.

The velocity outside both boundary layers has a relatively simple structure. Batchelor (1956) has shown that inside any closed streamline, the potential vorticity ω/R is constant. This, however, does not fully determine the shape of the velocity field in the core region as we cannot rule out the possibility of more than one region of closed streamlines existing. Indeed, this we find often to be the case.

Now outside the viscous layer (3.7) reduces to

$$u.\nabla\left(\frac{\omega}{R}\right)=O(Re^{-1}), \tag{3.15}$$

which implies ω/R is constant along streamlines. This standard result for axisymmetric, high-Reynolds-number flows is illustrated by the numerical experiments for the sphere in §6. If we introduce a stream function Ψ such that $\mathbf{u}=\nabla\wedge(0,0,\Psi/R)$ and $\Psi=0$ on $n=0$ then we may write

$$\frac{\omega}{R}=f(\Psi), \tag{3.16}$$

where f is some function. In principle, f is determined by the streamline integrals

$$\oint_{\Psi=\Psi_0}\left(\nabla^2\mathbf{u}+\frac{1}{\delta_{\mathrm{m}}}\mathbf{F}\right).d\mathbf{l}=0. \tag{3.17}$$

Now (3.16) is incompatible, in general, with the stress-free condition in (2.11), and we therefore perceive the need of a viscous layer near the surface. This should be contrasted with the cylindrical problem considered by Jones, Moore & Weiss (1976) in their work on axisymmetric convection, in which the condition of vanishing stress is identical with one of vanishing vorticity, due to the straightness of the boundaries.

4. The high-surface-tension limit

As $W\to\infty$ in (3.8) it is evident that $K\to K_0$, and hence that the blob becomes almost spherical. In this limit, therefore, considerable progress can be made by means of a perturbation expansion. Unfortunately, except for very small drops ($a\sim 1$ mm),

for which some of our other assumptions become tenuous (for instance $\delta_m \ll 1$), this limit is not physically realized. Nevertheless, it is of value to consider it for two reasons. Firstly, since the perturbation is regular, we may expect it to remain qualitatively correct for $W = O(1)$, giving us a fair idea of the shape adopted by larger drops. But most relevantly, it is invaluable to have a way of examining the behaviour of the velocity field in various ranges of the parameters Re and δ_m for a given shape.

We use spherical polar co-ordinates (r, θ, ϕ) and define

$$\epsilon = \frac{\max(1, Re\,\delta_m)}{W} \ll 1. \tag{4.1}$$

Then (3.8) can be re-expressed in the form

$$K(\theta) - K_0 = \epsilon h_1(\theta) + \epsilon^2 h_2(\theta) + \dots, \tag{4.2}$$

where $h_i(\theta)$ are determinable functions once the ϵ^{i-1} problem has been solved. We represent the almost-spherical surface by

$$r = 1 + \epsilon R_1(\theta) + \epsilon^2 R_2(\theta) + \dots, \tag{4.3}$$

and then the curvature $K = \partial n_i / \partial x_i$ is given by

$$K = 2 - \epsilon L R_1 - \epsilon^2 \{L R_2 - 2 R_1 L R_1 + 2 R_1^2\} + \dots, \tag{4.4}$$

where L is the first Legendre operator defined by

$$L\chi = \frac{1}{\sin\theta} \frac{\partial}{\partial\theta} \left(\sin\theta \frac{\partial \chi}{\partial \theta} \right) + 2\chi. \tag{4.5}$$

If we now write $K_0 = K_{00} + \epsilon K_{01} + \epsilon^2 K_{02} + \dots$ then equating coefficients of ϵ^i gives

$$K_{00} = 2,$$

$$L R_1 + K_{01} = -h_1(\theta) \equiv -h_1^*, \tag{4.6}$$

$$L R_2 + K_{02} = -h_2(\theta) + 2 R_1 L R_1 - 2 R_1^2 \equiv -h_2^*, \tag{4.7}$$

and so on. We thus obtain second-order differential equations for the shape perturbations. One boundary condition comes from mass conservation:

$$\int r^3 \Big|_S \sin\theta \, d\theta = \text{constant}, \tag{4.8}$$

i.e.

$$0 = \int_0^\pi R_1 \sin\theta \, d\theta = \int_0^\pi (R_1^2 + R_2) \sin\theta \, d\theta = \dots. \tag{4.9}$$

Since the operator L contains a constant multiplier, we can absorb the constants K_{0i} into R_i and regard (4.9) as determining them.

Now $L\chi = 0$ has a general solution

$$\chi = C \cos\theta + D \cos\theta \log \frac{1 - \cos\theta}{1 + \cos\theta}, \tag{4.10}$$

and for regularity at $\theta = 0, \pi$ we must require $D = 0$ in any solution. This leads to a solvability constraint on h_i. For if χ is regular then since L is self-adjoint

$$\langle L\chi, \cos\theta \rangle = \langle \chi, L \cos\theta \rangle = 0, \tag{4.11}$$

where
$$\langle x, y\rangle = \int_0^\pi xy \sin\theta \, d\theta. \tag{4.12}$$

We thus have at ith order a secularity condition

$$\langle h_i^*, \cos\theta\rangle = 0, \tag{4.13}$$

which is requiring that the system should be in bulk equilibrium to $(i-1)$th order. This connection derives from the physically obvious fact that surface tension provides no net force on a closed isolated blob of fluid. The coefficients of the free solutions $C_i \cos\theta$ in (4.10) correspond to a shift in position of the entire blob through a distance $C_i \epsilon^i$, and must be chosen so that equilibrium between gravity and the levitation force is maintained to all orders.

If we write $\mathbf{B} = \nabla \wedge (0, 0, A)$, then in the absence of the sphere we may expand

$$A = \sum_{n=1}^{\infty} A_{n0} r^n P_n^1(\cos\theta), \tag{4.14}$$

where P_n^1 is an associated Legendre function, and the coefficients A_{n0} may be calculated in terms of the known external current distribution. For a current loop at $r = r_0$, $\theta = \theta_0$, for example,

$$A_{n0} = \frac{1}{n(n+1)} \frac{\sin\theta_0}{r_0^n} P_n^1(\cos\theta_0), \tag{4.15}$$

and we may superpose such fields as required. In the presence of the sphere the field is given by

$$A = \sum_{n=1}^{\infty} A_{n0} \left(r^n - \frac{1}{r^{n+1}} \right) P_n^1. \tag{4.16}$$

If we now perturb the sphere and expand $A = A_0 + \epsilon A_1 + \ldots$ then A_0 is given by (4.16). A_i may be expanded

$$A_i = \sum_{n=1}^{\infty} A_{ni} r^{-(n+1)} P_n^1, \tag{4.17}$$

and the boundary condition that A vanishes on S implies

$$\sum_{n=1}^{\infty} A_{n1} P_n^1 + R_1(\theta) \frac{\partial A_0}{\partial r}\bigg|_{r=1} = 0, \tag{4.18}$$

and so on. In the numerical experiments to follow we do not calculate more than the first perturbation, and so from now on we ignore terms of order less than ϵ. Then from (1.3) and (4.18)

$$A_{n1} = \frac{-(2n+1)}{2n(n+1)} \int_0^\pi \sin\theta \, R_1(\theta) \, B_{s0}(\theta) \, P_n^1(\cos\theta) \, d\theta. \tag{4.19}$$

The perturbed field now being known, we may calculate the magnetic pressure on the perturbed surface. The requirement that the levitation force is unchanged to order ϵ then gives

$$\int_0^\pi \{B_{s0}^2 [2R_1 \sin\theta \cos\theta + R_1' \sin^2\theta] + 2B_{s0} B_{s1} \sin\theta \cos\theta\} \, d\theta = 0. \tag{4.20}$$

This relation fixes the value of the coefficient C_1 and thus completes the determination of R_1.

To first order, we solve the above perturbation problem numerically in three steps:

(i) find the surface field on a conducting sphere with the given external current distribution of sufficient strength to support it;

(ii) solve the Navier–Stokes equations in the sphere driven by the associated Lorentz force;

(iii) derive the corresponding surface perturbation.

In §5 we outline the numerical techniques used.

5. Numerical methods

We rewrite (2.6), (3.7) by introducing a stream function Ψ such that $\mathbf{u} = \nabla \wedge (0, 0, \Psi/r\sin\theta)$, and allowing for time dependence, in the form

$$\frac{\partial \omega}{\partial t} = \frac{1}{r\sin\theta} D^2(\omega r \sin\theta) + \frac{1}{\delta_m} \exp\left(\frac{r-1}{\delta_m}\right) G(\theta) + \frac{Re}{r} \frac{\partial(\Psi, \omega/r\sin\theta)}{\partial(r,\theta)} \tag{5.1}$$

$$-\omega r \sin\theta = D^2\Psi, \tag{5.2}$$

where the Stokes operator

$$D^2 \equiv \frac{\partial^2}{\partial r^2} + \frac{1}{r^2\sin^2\theta}\frac{\partial^2}{\partial\theta^2} - \frac{\cot\theta}{r^2}\frac{\partial}{\partial\theta},$$

and the last term in (5.1) is a Jacobian. We wish to solve (5.1), (5.2) in the sphere $r = 1$, with boundary conditions

$$\left.\begin{aligned} \Psi &= 0, \\ \omega\sin\theta &= -2\frac{\partial\Psi}{\partial r}. \end{aligned}\right\} \quad \text{on} \quad r = 1 \tag{5.3, 5.4}$$

Various sophisticated techniques have been developed for the solution of this type of equation (Weir 1976; Jones *et al.* 1976), but owing to the relative simplicity of the problem we use a naive second-order finite-difference scheme. We define a regular circular grid and time-step towards equilibrium using a Dufort–Fraenkel centred scheme. Each time step we use (5.1) to find the new vorticity distribution inside the sphere. We then solve (5.2) with (5.3) by relaxation for the new stream function, and finally use (5.4) to find the surface vorticity. Equilibrium is defined to be when $\max\{\omega^{-1}\partial\omega/\partial t\} < \epsilon^*$ for some suitably small ϵ^*. Because of the boundary-layer structure of the solution, computational efficiency suggests that more points should be placed near the surface. It is a simple matter to halve the mesh spacing above a given radius without loss of accuracy.

The scheme sketched above can be tested by inputting an artificial forcing G, for which there exists an analytic solution for (Ψ, ω). Varying the step lengths then demonstrates that the scheme is indeed second-order and converges as the step length tends to zero.

To find the actual forcing we use a truncated series of associated Legendre functions. The truncation length was chosen such that the proportional change in the surface field on increasing the number of included terms was significantly less than the second-order errors of the finite-difference scheme. At each grid point on the surface,

(4.16), together with the recurrence relation

$$\left.\begin{aligned}(2n+1)\cos\theta P_n^1 &= nP_{n+1}^1+(n+1)P_{n-1}^1,\\ P_0^1 = 0, \quad P_1^1 &= \sin\theta,\end{aligned}\right\} \tag{5.5}$$

was used to obtain the value of B_s. The results were checked against a more-general integral-equation method. The function $G(\theta)$ is then found from $B_s(\theta)$ by differences.

Once the flow field has been found, the surface perturbation can be calculated by inverting the differential operator L in (4.6). If we write

$$R_1 = -\tfrac{1}{2}K_{01}(1-\cos\theta)+R_1(0)\cos\theta+S_1, \tag{5.6}$$

then we are left with the problem

$$LS_1 = -h_1(\theta), \quad S_1(0) = S_1'(0) = 0. \tag{5.7}$$

If we now express the operator L in difference form it is possible to 'shoot' from $\theta = 0$ to $\theta = \pi$ without picking up the logarithmically singular solution. The accuracy can be tested by shooting backwards with the obtained solution. Application of the boundary conditions (4.9) and (4.20) then determines the constants $R_1(0)$ and K_{01}, and defines the surface perturbation uniquely.

In §6 we describe the solutions obtained by the above methods.

6. Numerical results

Solutions have been obtained for various coil configurations and values of Re and δ_m. Those presented here pertain to the fields shown in figure 2. The 'single-loop' configuration has the numerical advantage of structural simplicity, but in practice a blob levitated by such a device is unstable to vertical oscillations. The 'basket' design, with the characteristic counterwound 'lid', is a closer model of a realistic levitation device.

The driving function $G(\theta)$ changes sign at extrema of the surface field B_s, and is therefore quite complex in general. As a result, at low Reynolds numbers many gyres may form, but as Re is increased for fixed δ_m, it is found that one dominant gyre emerges, swallowing up all but a small remnant near the bottom. This is not surprising since for high Reynolds number the Lorentz force appears only in the streamline integral of (3.17), and thus its local structure is less important.

For the single-loop field, figure 3 describes the solution for $Re = 400$, $\delta_m = 0{\cdot}05$. The streamlines (right) are plotted alongside the contours of ω/R (left) for comparison. In each case 15 contours are drawn between the maximum and minimum values, and thus the weak gyre at the bottom of the fluid has not shown up on the streamline diagram. It is evident from figure 3 firstly that outside both boundary layers there is a plateau of potential vorticity, and secondly, away from this plateau, that ω/R is approximately constant along streamlines, in keeping with the theoretical results at the end of §3. In figure 4, 3 solutions are plotted for the basket-field case. The plateau area is less distinct for the relatively high value of δ_m shown in figure 4(*a*), though the contours show similar tendencies. The character of the flow is markedly different, however, when $\delta_m \ll \delta_v$. In this limit, it is possible to integrate across the magnetic layer and proscribe a magnetic surface stress instead of the Lorentz force. In figure

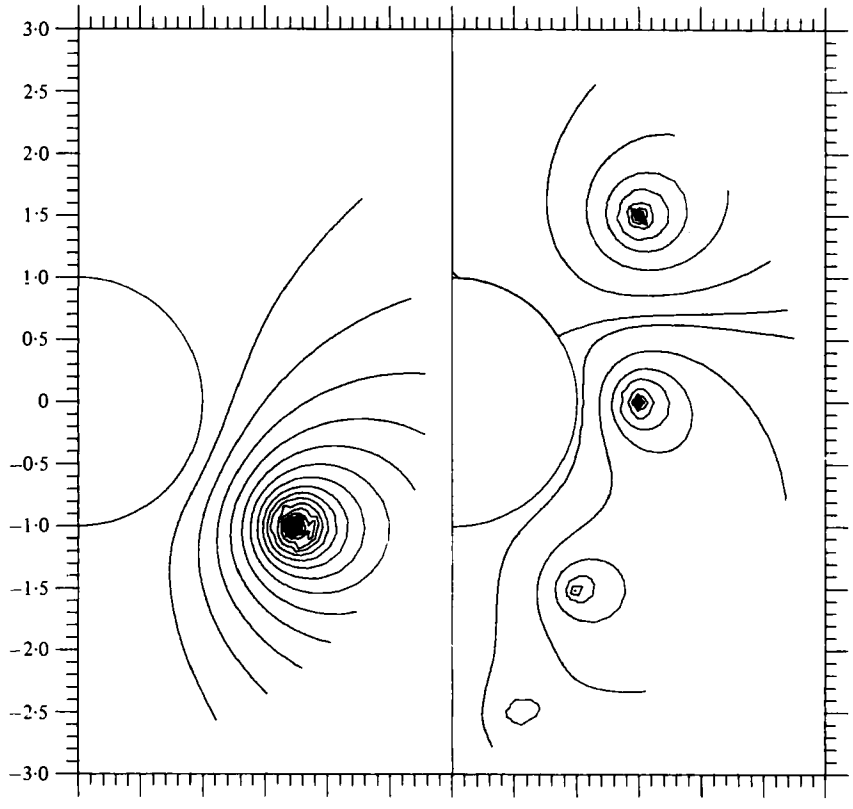

FIGURE 2. Magnetic field lines: (*a*) 'single-loop' coil at $(R, z) = (1{\cdot}732, -1)$; (*b*) 'basket' coils at $(R, z) = (0{\cdot}5, -2{\cdot}5)$, $(1, -1{\cdot}5)$ and $(1{\cdot}5, 0)$, counterwound coil at $(R, z) = (1{\cdot}5, 1{\cdot}5)$.

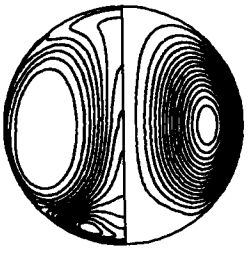

FIGURE 3. 'Single-loop' flow solution for $Re = 400$, $\delta_m = 0{\cdot}05$; streamlines on right; contours of potential vorticity on left.

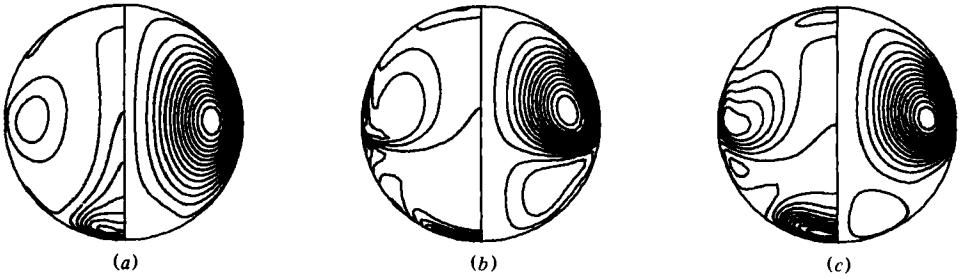

(*a*) (*b*) (*c*)

FIGURE 4. 'Basket' flow solutions: (*a*) $Re = 300$, $\delta_m = 0{\cdot}125$; (*b*) $Re = 250$, $\delta_m \to 0$; (*c*) $Re = 125$, $\delta_m = 0{\cdot}05$.

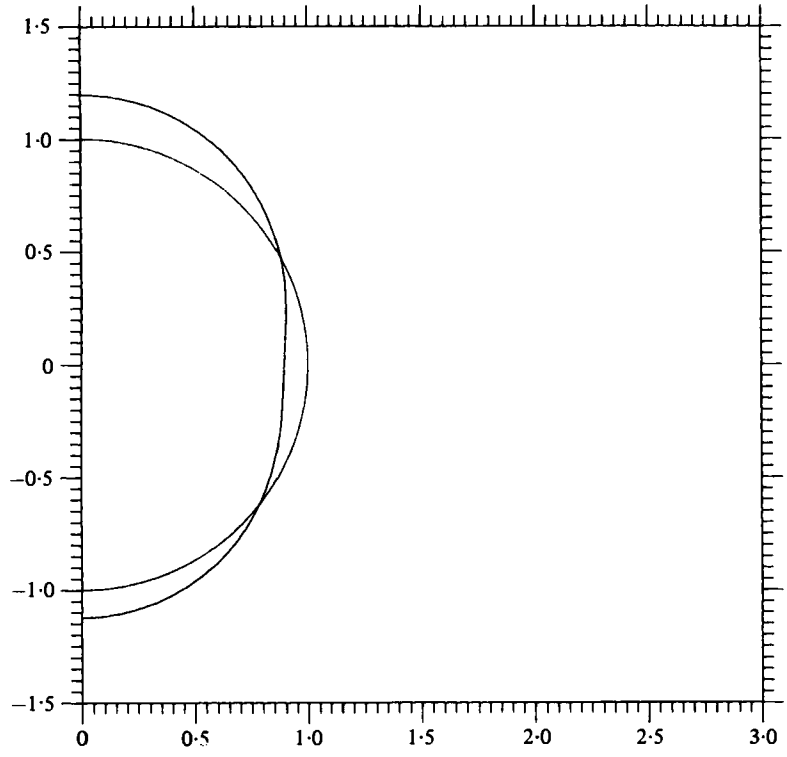

FIGURE 5. Surface perturbation for 'basket'. $Re = 300$, $\delta_m = 0{\cdot}125$, $\epsilon = 1$.

4(*b*) two gyres are clearly visible, each with an associated value of constant potential vorticity outside the complex viscous layer. This pattern persists as the Reynolds number is increased. In figure 4(*c*) $\delta_m \sim \delta_v$, and all streamlines pass through the boundary layer. In this intermediate case an involved structure of ω/R results, fully dependent on the form of $G(\theta)$.

The surface perturbations associated with the above cases are qualitatively similar, and figure 5, corresponding to figure 4(*a*), is typical. The curvature increase at the bottom required by (2.14) is apparent, while comparison with figure 2 indicates a tendency for the fluid to move preferentially into regions of weak field. The perturbation is plotted for $\epsilon = 1$ to aid resolution.

The tendency of the smaller gyre to shrink with increasing Re enables us to calculate the asymptotically constant value of the potential vorticity in the larger gyre. For if we write $\omega/R = \beta$ throughout the core, then the core flow is given by the stream function

$$\Psi = \tfrac{1}{10}\beta(r^2 - r^4)\sin^2\theta. \tag{6.1}$$

Substituting this velocity field in the right-hand side of (3.5), and recalling that the velocity is approximately constant across the magnetic layer, we obtain

$$2\int_{r\leq 1} e_{ij}e_{ij}\,dV = \tfrac{4}{25}\beta^2 2\pi + O(\delta_m). \tag{6.2}$$

The left-hand side of (3.5) can be written

$$\int \mathbf{u}.\mathbf{F}\,dV = -2\pi\int_0^{\pi} d\theta \int_0^{-\infty} dn\tfrac{1}{2}B_s^2 e^n u_n \sin\theta$$

$$= -\tfrac{2}{5}\pi\beta\int_0^{\pi} B_s^2 \sin\theta\cos\theta\,d\theta + O(\delta_m) \tag{6.3}$$

Combining (6.2) and (6.3) yields

$$\beta = -\frac{5}{4}\int_0^{\pi} B_s^2 \sin\theta\cos\theta\,d\theta, \tag{6.4}$$

or

$$\beta = -\frac{5}{6\alpha}, \tag{6.5}$$

since the right-hand side of (6.4) is proportional to the total lift. Thus as pointed out privately by Sneyd, the value of β is independent of the coil arrangement! This last result holds only for a spherical shape, however. The 'plateau' value in figure 3 agrees quite well (within 2 %) with the theoretical value of β given by (6.5).

7. Concluding remarks

The high-Weber-number limit has physical significance only for small drops of fluid ($a \sim 1$ mm). Nevertheless, it gives useful insight into the fluid behaviour in the three regions of the flow, which one would expect to be qualitatively similar inside a more generally shaped surface whenever the Lorentz force is balanced by the viscous forces. This work suggests that as the Reynolds number is increased a single gyre will emerge with an associated constant value of ω/R. This value may be calculated by the techniques of § 6 to give

$$\frac{\omega}{R} = \frac{\int_0^{s(\text{top})} RUB_s \dfrac{\partial B_s}{\partial s}\,ds}{2\displaystyle\int_V E_{ij}E_{ij}\,dV}, \tag{7.1}$$

where $U(s)$ is the surface velocity, and E_{ij} the rate-of-strain tensor for unit potential vorticity throughout V. For a spherical shape, this value is zero only if the levitation force vanishes, but in general, it may happen that

$$\int_0^{s(\text{top})} RUB_s \frac{\partial B_s}{\partial s}\,ds = 0. \tag{7.2}$$

We find numerically that the flow in a sphere driven by a uniform external field (for which (7.2) holds) consists of two symmetric gyres even for large Re. By analogy, we expect that if (7.2) holds for a given shape, then a two-gyre pattern will persist as $Re \to \infty$, but otherwise a single gyre of strength given by (7.1) will emerge.

There is a strong indication that the asymptotic limits $Re \to \infty$ and $\delta_m \to 0$ are not interchangeable for a given configuration. When $Re \to \infty$ first, the core flow becomes a single gyre of constant ω/R, whereas if we first let $\delta_m \to 0$ two gyres of comparable size with positive and negative ω/R form. However, these limits require different surface boundary conditions, and when $W = O(1)$ will not, in general, give rise to the same shape.

In the limit $\delta_m \to 0$ it can be shown that the dynamics do not effect the surface shape and solutions have been obtained for $W = O(1)$ by a different approach. When $Re \to \infty$ for $W = O(1)$ the condition (3.13) fails. Sneyd & Moffatt (1982) consider it unlikely that a laminar solution exists in this limit, but it may be that a boundary-layer approach similar to that of Fautrelle (1981) will lead to a solution based on the free-fall velocity scale. This idea is being investigated.

REFERENCES

Batchelor, G. K. 1956 On steady laminar flow with closed streamlines at large Reynolds number. *J. Fluid Mech.* **1**, 177.

Fautrelle, Y. R. 1981 Analytical and numerical aspects of the electromagnetic stirring induced by alternating magnetic fields. *J. Fluid Mech.* **102**, 405.

Harris, M. R. & Stephan, S. Y. 1975 Support of liquid metal surface by alternating magnetic field. *I.E.E.E. Trans. on Magnetics* **5**, 1508.

Jones, C. A., Moore, D. R. & Weiss, N. O. 1976 Axisymmetric convection in a cylinder. *J. Fluid Mech.* **73**, 353.

Moffatt, H. K. 1965 On fluid flow induced by a rotating magnetic field. *J. Fluid Mech.* **22**, 521.

Moffatt, H. K. 1977 Some problems in the magnetohydrodynamics of liquid metals. *Z. angew. Math. Mech.* **58**, 65–71.

Muck, O. 1923 *German Patent* no. 422004, *Oct.* 30, 1923.

Okress, E. C., Wroughton, D. M., Comenetz, C., Brace, P. N. & Kelly, J. C. K. 1952 Electromagnetic levitation of solid and molten metals. *J. Appl. Phys.* **23**, 545.

Peifer, W. A. 1965 Levitation melting . . . a survey of the state-of-the-art. *J. Metals* **17**, 487.

Polonis, B. M. & Parr, J. G. 1954 Phase transformations in titanium rich alloys of iron and titanium. *Trans. A.I.M.E.* **200**, 1148.

Sagardia, S. R. 1977 Electromagnetic levitation melting of large conductive loads. Ph.D. thesis, University of Toronto.

Sneyd, A. D. 1979 Fluid flow induced by a rapidly alternating or rotating field. *J. Fluid Mech.* **92**, 35.

Sneyd, A. D. & Moffatt, H. K. 1982 Fluid dynamical aspects of the levitation-melting process. *J. Fluid Mech.* **117**, 45.

Weir, A. D. 1976 Axisymmetric convection in a rotating sphere. Part 1. Stress-free surface. *J. Fluid Mech.* **75**, 49.